Available online at www.sciencedirect.com
SCIENCE DIRECT®
International Journal of Thermal Sciences 44 (2005) 894–902
International Journal of Thermal Sciences
www.elsevier.com/locate/ijts

Experiments of fluid flow and heat convection in the wake of a disk facing a uniform stream

Abdullah Abbas Kendoush [a,*], Akram Wahbi Izzat [b]

[a] *Department of Heat Transfer, Centre of Engineering Physics, Division of Physical Sciences and Research, Ministry of Sciences and Technology, Baghdad, Iraq*

[b] *Department of Mechanical Engineering, College of Engineering, University of Baghdad, Baghdad, Iraq*

Received 12 April 2004; received in revised form 5 January 2005; accepted 11 February 2005

Available online 31 March 2005

Abstract

An experimental investigation on the fluid flow and heat convection from the wake region of a circular disk was performed. The flow experiments covered the range of Reynolds numbers from 1.4×10^3 to 5×10^4. The local flow velocity was measured in a water channel. Two different methods were used for these measurements, a thermistor and a Pitot tube. These measurements were supported by flow visualization using the hydrogen bubble generation technique. The convective heat transfer from the disk was measured in an air stream coming out of a wind tunnel. The heat transfer measurements covered a range of Reynolds number from 2.2×10^4 to 5.3×10^4. The local heat transfer coefficients along the radius of the disk were measured at 5 positions for both the front and wake regions. An electrically heated disk was used for these measurements. The local heat transfer coefficient showed a radial distribution with a maximum at the edge of the disk and a minimum at the center.

Keywords: Heat convection; Fluid flow; Circular disk; Wake region

1. Introduction

The applications of circular disks in mechanical, chemical and aeronautical engineering are quite common. The experimental efforts of this investigation were focused on the fluid flow in the wake of the disk and the convective heat transfer from both sides of the disk, namely, the upstream side facing the flow and the wake side.

The research on the wake of the disk dates back to 1930 when Marshall and Stanton [2] observed a permanent vortex ring at Reynolds number ranging from 5 to 195. Taylor [3] derived the fundamental parameters of this ring, e.g. the radii of the core and the cross section.

Carmody [4] reported velocity measurements obtained in the wake and demonstrated that flow separation at the edge of the disk leads to the formation of a recirculation zone that closes behind the disk at about two to three diameters downstream. The circulation zone results in an intensive fluid mixing which has a profound effect on the rates of heat, mass and momentum transfer.

Calvert [5] measured the pressure distribution in the wake of an inclined disk. The pressure distribution was presented as a function of distance from the disk. Vincent [6] utilized the circulation of the wake for the development of the electrostatic dust precipitator.

Miyagi and Kamei [7] found out theoretically that the critical Reynolds number at which a standing vortex first appears behind the disk is zero and the flow separates from the edge of the disk.

The available literature on forced convective heat transfer to a disk facing a uniform and perpendicular flow included three papers, respectively by Sogin [8], Beg [9] and Sparrow and Geiger [10]. In all these papers, the naphthalene sublimation technique, a mass transfer method, was employed to

* Corresponding author. Mailing address: PO Box 28432, 12631 Baghdad, Iraq.

E-mail address: kendoush@yahoo.com (A.A. Kendoush).

1290-0729/$ – see front matter
doi:10.1016/j.ijthermalsci.2005.02.005

Nomenclature

A	area	m^2	
a	disk radius	m	
D	disk diameter	m	
h	heat transfer coefficient at the upstream side of disk	$W \cdot m^{-2} \cdot K^{-1}$	
I	electric current	A	
k	thermal conductivity of fluid	$W \cdot m^{-1} \cdot K^{-1}$	
Nu	average Nusselt number, $2ah/k$		
Nu^*	average Nusselt number, ah/k		
$Nu(r)$	local Nusselt number, $2ah(r)/k$		
Pr	Prandtl number, $\mu C_p/k$		
Q	heating rate	W	
r	radial coordinate	m	
R	electric resistance	Ω	
Re	Reynolds number at the upstream side of disk, $2aU/\nu$		
Re_w	Reynolds number at the wake, $2aU_w/\nu$		
Re^*	Reynolds number, aU/ν		
$T_{s,a}$	temperature of disk surface and air respectively	°C	
U	main upstream velocity	$m \cdot s^{-1}$	
U_w	main reverse velocity of the wake	$m \cdot s^{-1}$	
V_r	radial component of the flow velocity in the wake	$m \cdot s^{-1}$	

Subscripts

o	conditions at the stagnation point of the upstream side of disk
w	conditions at the wake
o, w	conditions at the rear stagnation point

determine the heat transfer parameters. As far as the authors are aware, there were no reported works on direct heat transfer measurements from a circular disk. However, the three papers concentrated on the forced convection from the upstream side of the disk.

The prime motive behind the present research was to improve knowledge of the fluid flow around the disk and to probe directly into the thermal field of the disk with the intention of obtaining the relevant forced convective heat transfer variables from the wake side of the disk.

2. Experimental apparatus and procedure

2.1. Fluid flow measurements

The investigations were performed in an experimental test system, which was available in the College of Engineering. The system was a water channel of 0.3 m × 0.3 m × 10 m dimensions as shown in Fig. 1. The tested disks were glass of 3 mm thickness with two different diameters 0.0625 m and 0.075 m mounted broad side in the water channel. The disks

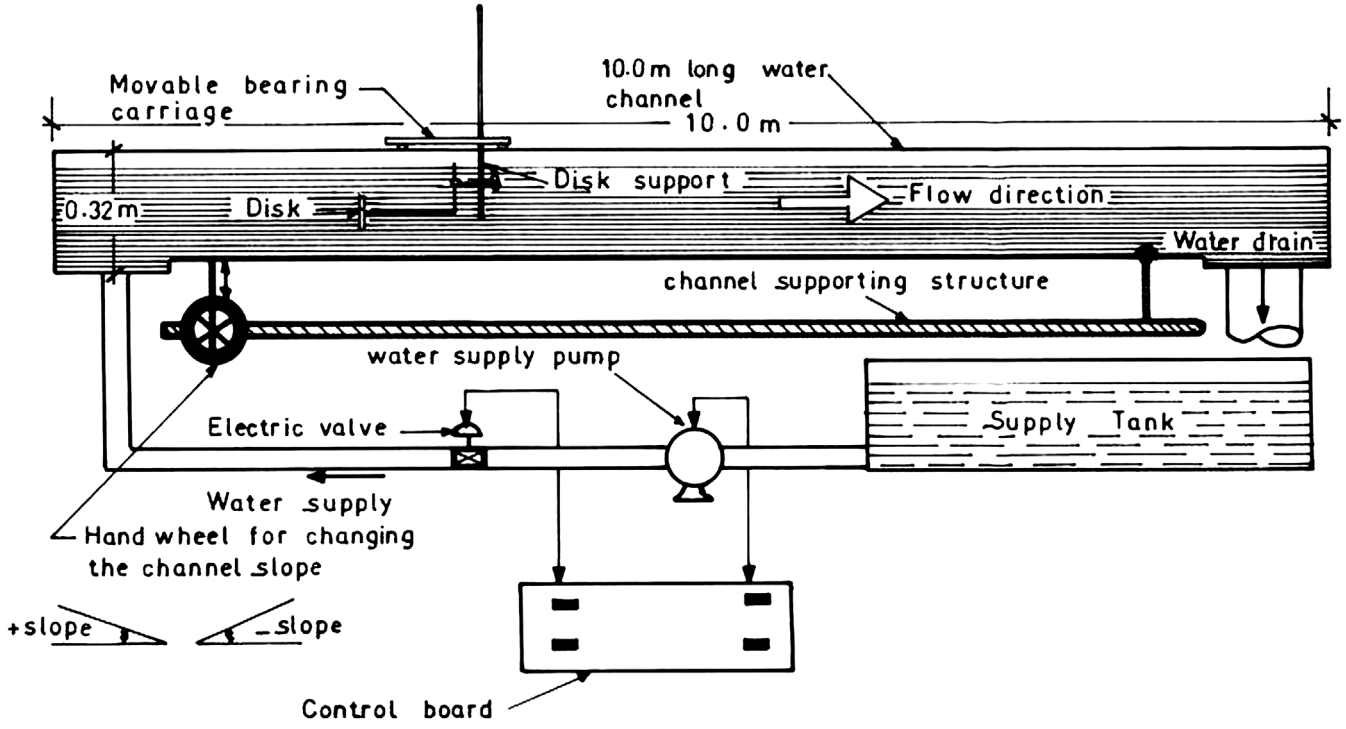

Fig. 1. The 0.3 m × 0.32 m × 10 m water channel used for conducting the flow experiments.

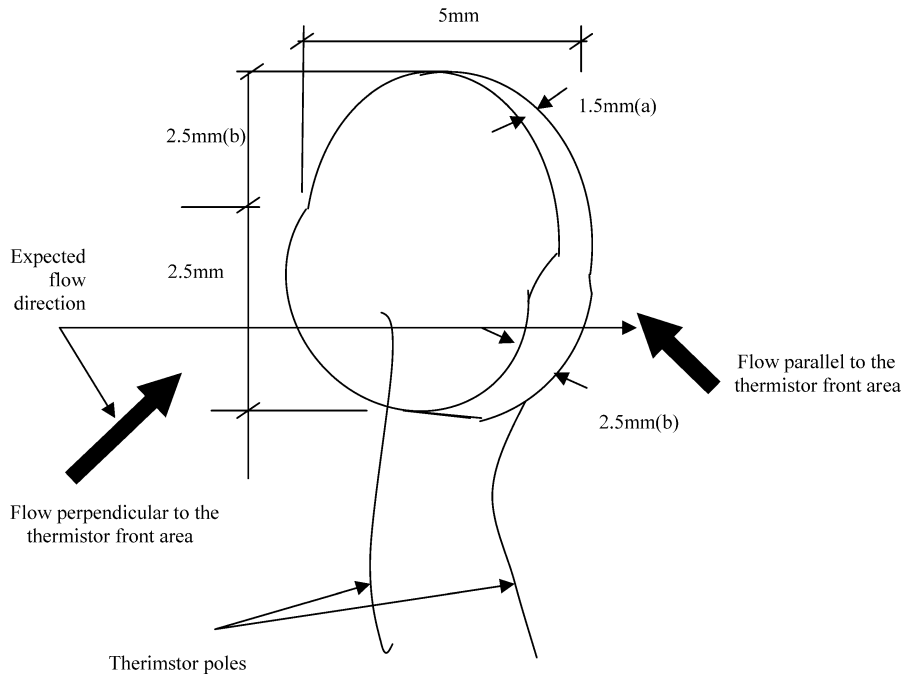

Fig. 2. The thermistor used for fluid velocity measurements.

were square-edged. The velocity of the water in the channel ranged from 0.05 $m \cdot s^{-1}$ to 0.5 $m \cdot s^{-1}$.

The magnitude of the velocity was measured by a thermistor (Kanbour [11]), which depends on the convective heat transfer between the surrounding fluid and the thermistor. The dissipation of heat does not depend on the direction of the flow due to the complicated geometry of the thermistor (see Fig. 2). Measurements were made by exerting an electrical potential through the sensing part of the thermistor and measuring the current passing through it. The thermistor, which is used in the experiments conducted in the water channel, was coated with a thin layer of nail paint to prevent current leakage to water. The electronic circuit of the thermistor was made according to the British standards B.S.1041 [12]. The device was calibrated in a special system to an accuracy of $\pm 1.98\%$. The calibration system and method are described in Appendix A.

The circular disks were mounted in the water channel by using L-shaped thin mechanical supports as shown in Fig. 1. The position and shape of these supports were carefully chosen to minimize flow perturbations (Izzat [13]). The measurements were taken at the same meridian plane. It was found that the water local velocity in different radial positions on the surface of the disk was symmetrically the same.

Flow visualization in the wake region performed using hydrogen bubble generation technique in the water channel. Small bubbles of the order of 0.10 mm dia. were generated at a chosen location to mark streamlines in the flow. An electronic circuit designed for the present experiment (see Fig. 3) was slightly different from that used by Schraub et al. [14]. The new circuit was characterized by a variable voltage power supply. This provided suitable working conditions of variable electrolyte concentrations and variable distances between electrodes at a constant frequency to get successive rows of bubbles separated by constant duration times.

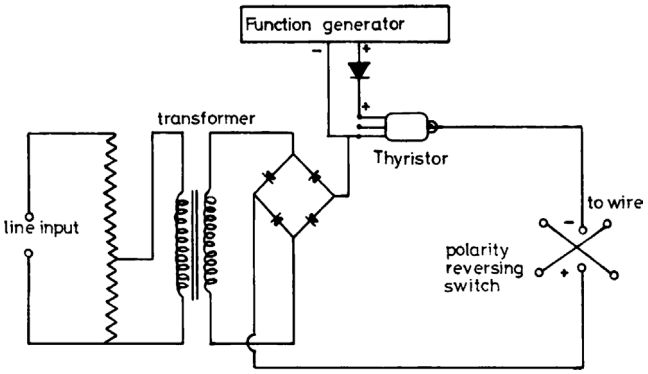

Fig. 3. The new electronic circuit utilized in the present flow experiments.

A power supply (Philips, Holland) of 75 V and 14 A was used together with a thyristor for voltage cutoff. The trigger voltage was supplied by means of (1 mHz–10 MHz) function generator (Philips, Holland) with $\pm 1\%$ accuracy in the megahertz range.

About 0.15 $g \cdot l^{-1}$ of Na_2SO_4 was added to the tap water to produce an electrolyte with sufficient number of ions. Fine copper and nichrome wires of (0.01–0.05) mm diameter were used as the negative electrodes while the positive electrode was the metallic disk support. It was found that these wires require aging under operating conditions for a few minutes before they produce bubbles uniformly.

A light source of 1000 W was fixed at 30 cm from the channel wall with a slot of 1 cm $\times$ 30 cm which was cut

through a wooden barrier to provide a collimated sheet of light for bubble photography by a camera of (Zenit, Russian made) (Izzat [13]).

The important factor, which limits the voltage required for good visualization, was the water velocity. It was found that the maximum operating voltage was 25 V for a water velocity range of (0.0216–0.0864) $m \cdot s^{-1}$.

2.2. Heat convection measurements

The heat transfer experiments were performed in the wind tunnel facility. Fig. 4 shows the details of the heated disk. Seven electrical coils, the resistance of each was 23.8 Ω, were prepared from 0.06 mm copper wires. To ensure homogeneous heat flux from the surface of the disk, the following were implemented:

- The heat-generated copper wires were distributed in a mesh of equal distances as shown in Fig. 4.
- Thin aluminum foils were wrapped around the copper wires.

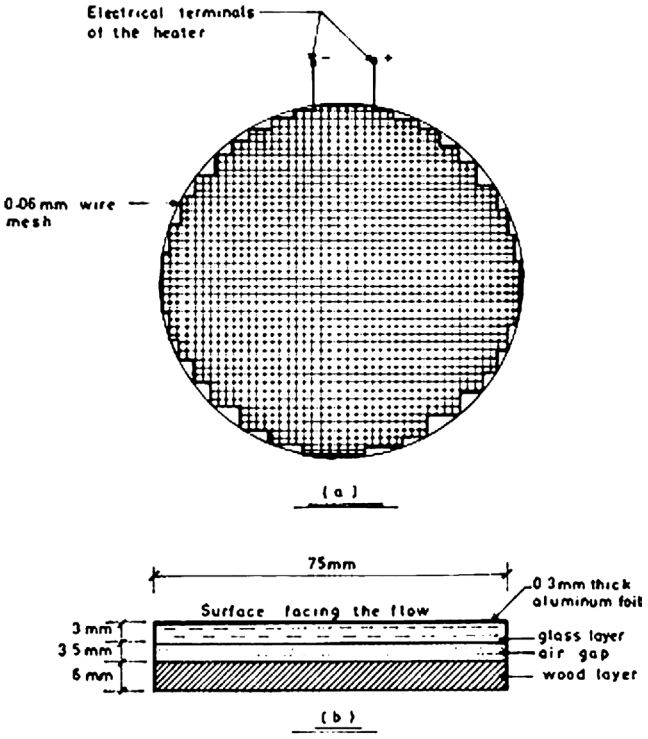

Fig. 4. (a) Hot plate fabricated from equally spaced wire mesh wrapped longitudinally and laterally around thin aluminum foil. (b) Multi-layer thermally insulated circular disk used in heat transfer measurements.

Another aluminum foil of 0.3 mm thickness was stuck to the heated one to ensure smooth surface. The heat transfer occurs from the copper wires to the first aluminum foils and then to the second aluminum foil. The other surface of the disk was insulated with 3.5 mm air gap and 6 mm wood layer. Special glue was used to keep these layers fixed. An electrical potential of 6.5 V was applied from a D.C. power supply to the coils.

The surface temperature of the heated disk was measured at five equally spaced radial positions of the 0.075 m diameter disk using calibrated thermistors. The experiments were performed in the wind tunnel shown in Fig. 5 where the heated disk was placed at the exit of the tunnel to avoid any flow blockage effects.

Before starting the experiments, the homogeneity of the heat flux was checked by measuring the surface temperature in stagnant air using calibrated thermistors. These measurements were done with the heated disk in a horizontal position in order to ensure homogeneous natural convection from the entire surface.

The heat transfer coefficients of the upstream side of the disk were measured by facing the heated surface to the upstream flow, while the other surface of the disk was insulated. The same procedure was repeated for the measurements of these coefficients in the wake region by turning the disk by 180 deg. around its major axis so that the heated surface will face the flow of the wake.

The local heat transfer coefficient was calculated from the following equation

$$h(r) = \frac{Q}{A(T_s(r) - T_a)} \tag{1}$$

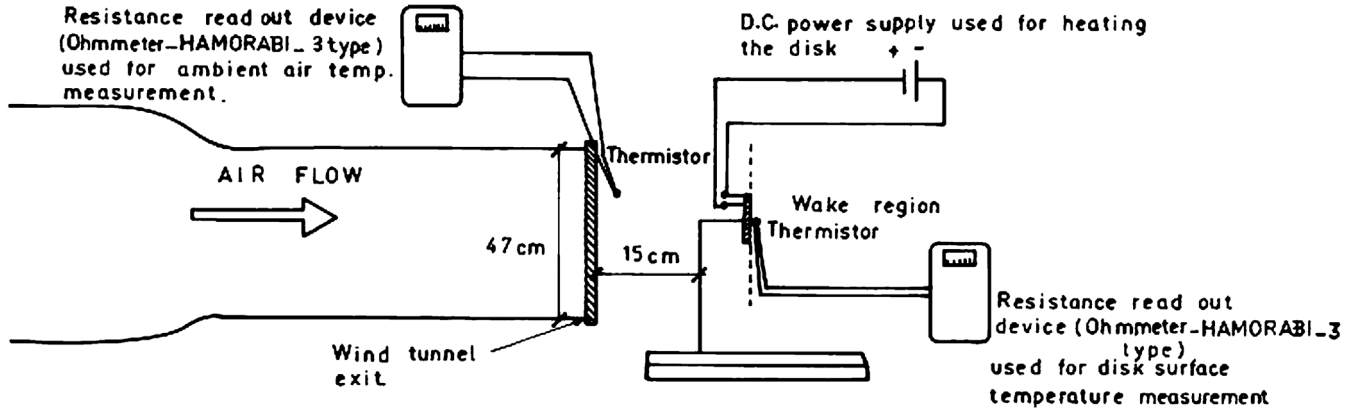

Fig. 5. Experimental system used for heat transfer measurements in both front and wake regions.

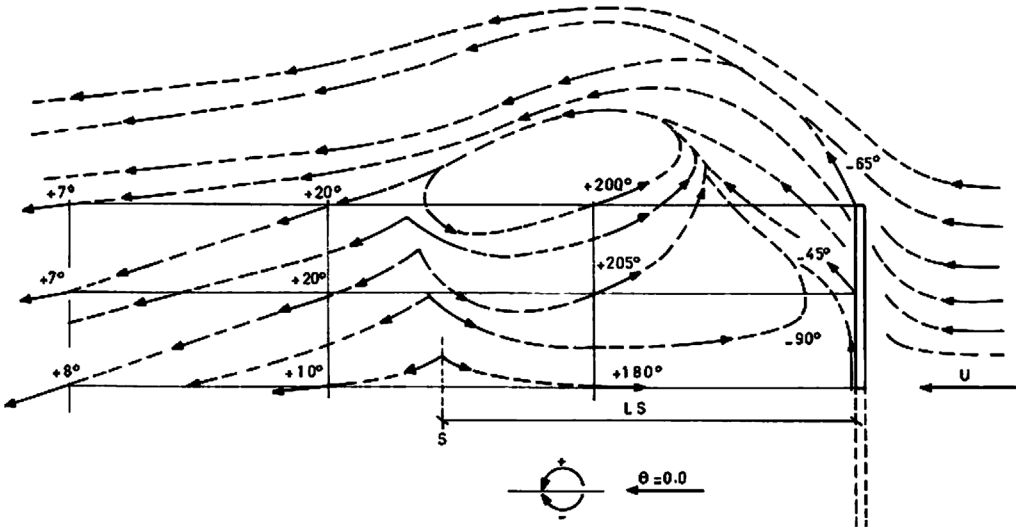

Fig. 6. Schematic diagram of the streamlines in the wake region of the circular disk based on the velocity directions measurements. The point S represents the separated flow, LS represents the distance between the rear centre of the disk and point S.

The heating rate was obtained from the electric resistance (that is, $Q = I^2R$). The average heat transfer coefficient was obtained according to the following:

$$h = \frac{2}{a^2}\int_0^a rh(r)\,\mathrm{d}r \tag{2}$$

It was found that the ambient air temperature was very close to the insulated surface temperature of the disk, which was measured at different positions. Thus, heat conduction through the insulation of Fig. 4 was neglected.

The careful and accurate calibration of the thermistor made the accuracy of the temperature difference measurement ranging from ±4% at $\Delta T = 13.7$ K to ±1% at $\Delta T = 11.9$ K.

The accuracy of the heat transfer coefficient measurement was ±2.0% at a confidence level of one standard deviation. It was calculated from $h = I^2R/(\pi a^2 \Delta T)$ by the following equation

$$\frac{\delta h}{h} = \left\{4\left(\frac{e_I}{I}\right)^2 + \left(\frac{e_R}{R}\right)^2 + 4\left(\frac{e_a}{a}\right)^2 + \left(\frac{e_{\Delta T}}{\Delta T}\right)^2\right\}^{1/2} \tag{3}$$

where e_I, e_R, e_a and $e_{\Delta T}$ are the uncertainties in the measurements of current, resistance, disk radius and temperature difference respectively.

3. Results and discussion

3.1. Fluid flow results

The following results were taken in the wake region of the disk. Fig. 6 shows the flow pattern in the wake region. The flow directions were measured with 3-hole Pitot tube. The flow pattern is illustrated in the hydrogen bubble photographs of the wake (Figs. 7 and 8). The flow is from right

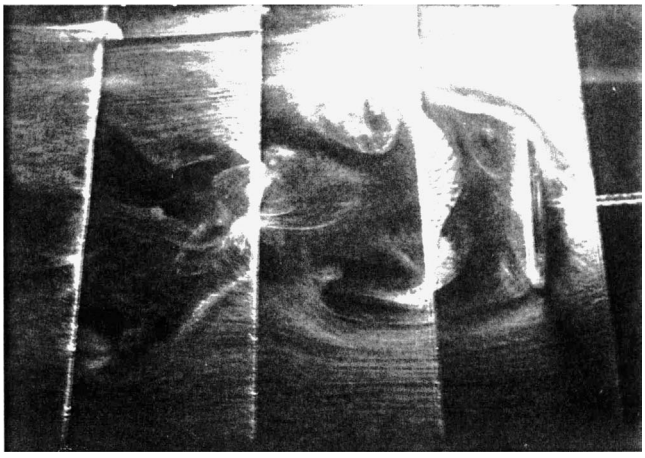

Fig. 7. The flow field of the wake region of the disk. The disk and its handle are situated to the right of the photograph. The flow is from right to left. The 4 vertical lines are the wires where hydrogen bubbles were generated. $Re = 1400$.

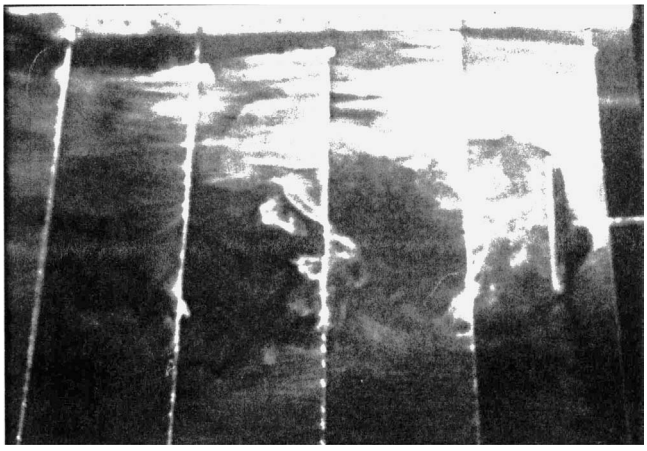

Fig. 8. The flow field in the wake region in the radial and axial directions. The disk and its handle are situated to the right. The flow is from right to left. $Re = 5615$.

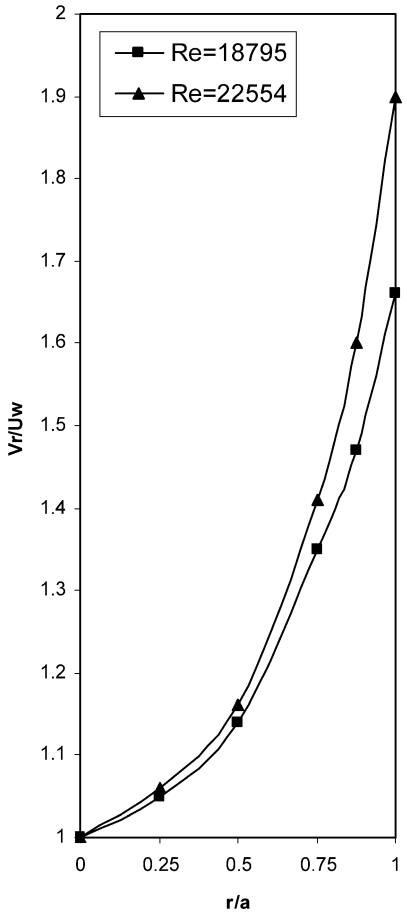

Fig. 9. The variation of the ratio V_r/U_w with r/a at different *Re* numbers near the surface of the disk in the wake region.

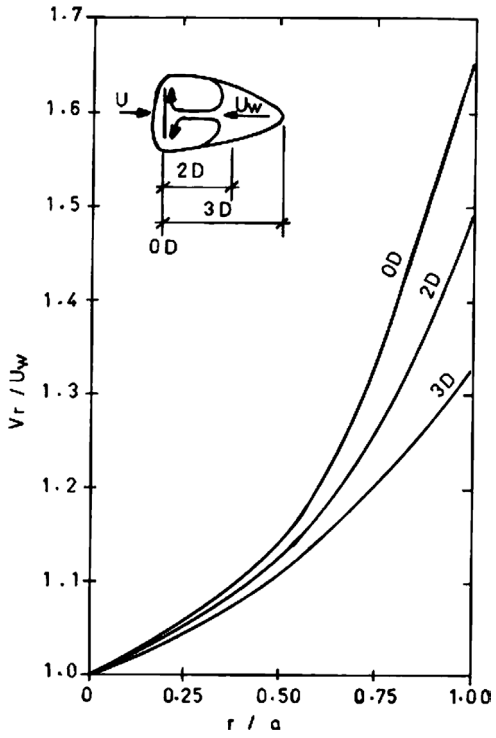

Fig. 10. The dependence of the velocity ratio V_r/U_w of the wake on the radial distance of the disk at different positions. $Re = 22554$.

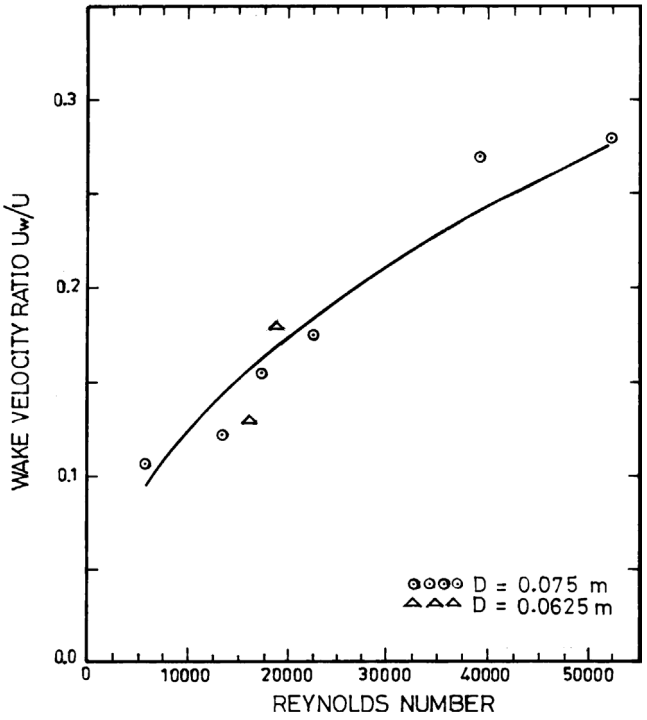

Fig. 11. Variation of the ratio of the main wake velocity to the main upstream velocity versus *Re* number.

to left. Note that the straight lines in the photographs are the nichrome wires that represent the cathode where the hydrogen bubbles are generated. The flow of water in the wake of the disk in Fig. 8 is at $Re = 5613$ where more vortices and turbulence are noticed as compared to that of Fig. 7 where $Re = 1400$.

Fig. 9 shows the increase of the ratio of the radial component of the velocity to the mainstream velocity of the wake (V_r/U_w) with the radial distance from the center of the disk. This increase causes a thinning of the momentum boundary layer towards the edge of the disk and a consequent increase in the heat transfer coefficient as will be explained in the next section (Fig. 16). The theoretical results of Kendoush [1] confirmed the above conclusion as the thermal boundary layer vanishes near the edge of the disk. The measurements of V_r/U_w at the wake were performed near the surface of the disk, at two and three diameters downstream from the surface as shown in Fig. 10. This indicates the existence of a steady reverse flow from the separation ring at the edge of the disk to the rear stagnation point.

Fig. 11 shows the variation of the ratio of the main reverse velocity of the wake to the upstream velocity with Reynolds number. The length scale used in *Re* number was the disk diameter. These results are useful in modeling the drag and heat convection in the wake. The present results are analogous to those of Lee and Barrow [15], which were utilized by Kendoush [16,17] in predicting the drag and heat convection from the wake of the sphere.

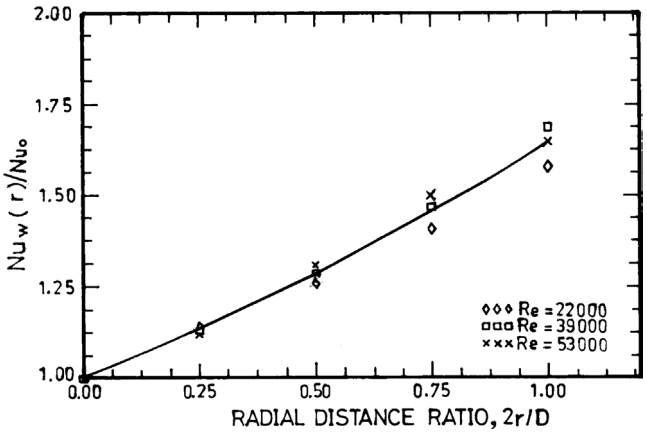

Fig. 12. Local *Nu* number to the stagnation point *Nu* number versus disk radial distance ratio in the wake region.

3.2. Heat transfer results

It was not possible to compare the present experimental results with the analytical solution of Kendoush [1] due to the different boundary conditions. The present experiment was based on constant heat flux conditions while the analyses were based on isothermal disk surface conditions.

The local variation of the ratio of Nusselt number to the Nusselt number at the stagnation point of the wake is shown in Fig. 12. These results are analogous to the fluid velocity results (Fig. 9). This is in qualitative agreement with the mass transfer results of Sparrow and Geiger [10]. They too found a similar profile for Sherwood number versus r/a but their mass transfer measurements were with Schmidt number of 2.55 while our data were with $Pr = 0.7$. The results of Fig. 12 indicate that *Nu* number is almost independent of the velocity of the flow. These results are analogous qualitatively to those of Murray et al. [20] who investigated the heat convection in the wake of a rectangular plate. The main justification of the increase in the heat transfer near the edge of the disk is the thinning of the boundary layer there due to the high speed of the fluid as seen in Fig. 9.

The present work at the wake of the disk complements that of Sparrow and Geiger [10] who studied heat and mass transfer from the upstream region of the disk.

The following experimental correlations of heat convection were obtained

$$Nu = 1.62Pr^{0.36}Re^{0.5} \tag{4}$$

for the average *Nu* at the upstream region and

$$Nu_w = 0.47Pr^{0.3}Re_W^{0.6} \tag{5}$$

for the average *Nu* at the wake region.

New correlations were obtained for the heat convection at the stagnation points as follows

$$Nu_o = 0.81Pr^{0.36}Re^{0.5} \tag{6}$$

at the upstream stagnation point and

$$Nu_{o,W} = 0.34Pr^{0.3}Re_W^{0.6} \tag{7}$$

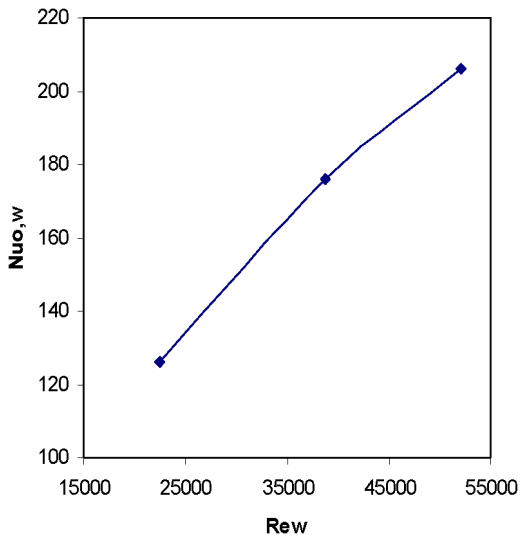

Fig. 13. Stagnation point *Nu* number versus *Re* number in the wake region of the disk.

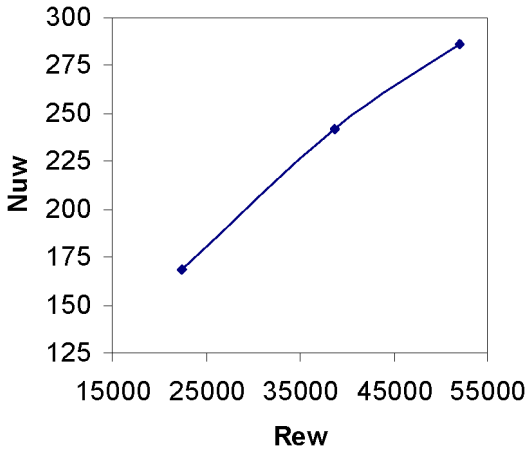

Fig. 14. The average *Nu* number versus *Re* number in the wake region of the disk.

at the rear stagnation point. The range of Reynolds number that covers equations (4)–(7) is from 22 000 to 52 000.

Figs. 13 and 14 show the variation of *Nu* number at the stagnation point of the wake and the average *Nu* with the *Re* number respectively. These are new data as far as the authors are aware. The increase of the rate of heat convection could be attributed to the increase in the speed of the reverse flow from the edge of the disk to the rear stagnation point. Fig. 14 shows the expected variation of the average *Nu* number with the *Re* number in the wake region of the disk.

Fig. 15 shows a comparison of the convective heat transfer at the stagnation points of a sphere and a disk. Although most of the experimental data and theoretical solutions were done at the forward stagnation point, the present results that were performed at the rear stagnation point fit in within the rest of the data comfortably. The theories of Kendoush [16], Sibulkin [18] and Short [19] and the experimental data of the indicated authors were shown in Fig. 15. Note that the dimensionless numbers were based on the radius of the disk

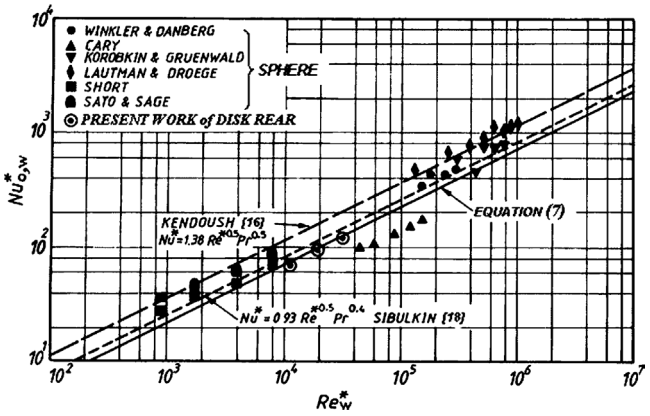

Fig. 15. Comparison of the present stagnation point heat transfer with those of the sphere of various authors. $Pr = 0.7$.

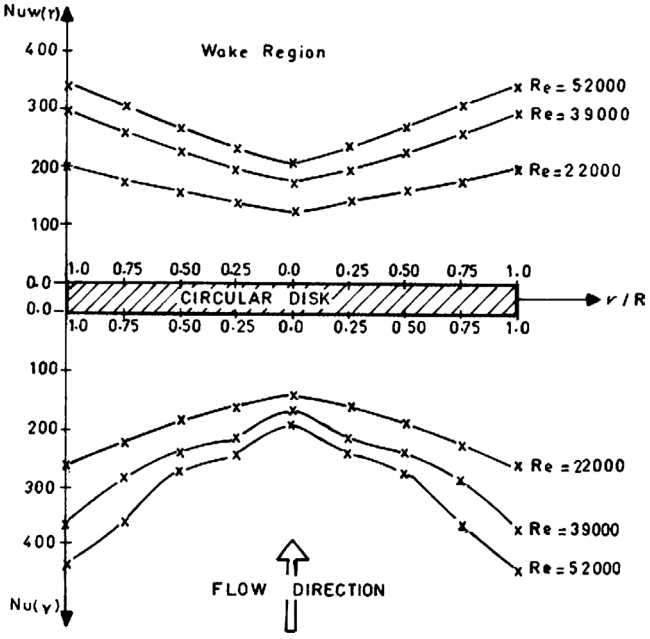

Fig. 16. Local variation of *Nu* number over the two broad surfaces of the disk of 7.5 cm dia. and 1.25 cm thickness versus the dimensionless radial coordinate.

and the sphere. Eq. (7) and the disk rear stagnation data are shown together with the sphere stagnation data of various investigators.

Fig. 16 shows a comparison between the local *Nu* number from the upstream side and the wake of the disk. Generally, higher values of *Nu* are shown in the upstream than the wake, due to higher values of the flow velocity at the upstream side of the disk than those of the wake.

4. Conclusions

An experimental study on the fluid flow and convection of heat from the wake of a disk leads to the following main conclusions:

(1) The radial component of the flow and the radial *Nu* increases with the radius of the disk.
(2) The main reverse velocity of the wake, the stagnation point *Nu* and the average *Nu* increase with *Re*.
(3) Reynolds number has no consistent effect on the radial distribution of heat convection rates.

Experimental correlations were obtained for the average, local, front and rear stagnation points heat convection rates from the disk. In general, higher rates of heat convection were recorded at the frontal surface of the disk than those at the rear surface.

Appendix A. Calibration method of thermistors

A.1. Thermistor characteristics

Plots of the electrical resistance of the thermistor at different temperatures were obtained by using a water bath with stirrer, a calibrated electronic thermometer and a digital Ammeter.

A.2. Theory of measurement and calculations

The theory of fluid velocity measurement using the thermistor is based on the convective heat transfer between the thermistor and the surrounding fluid. The average heat transfer coefficient h_t was obtained from the following equation

$$h_t = IV/A\Delta T \tag{A.1}$$

where

I is the electric current in the circuit, A,
V is the electric potential across the thermistor, V,
A is the themistor heat exchange area, m^2,
ΔT is the temperature difference between the thermistor and the surrounding fluid, K.

Due to the complicated shape of the thermistor as shown in Fig. 2, there is no empirical relationship between *Nu* number and *Re* number that fits this complicated shape, therefore we sought a relationship for this case of the following form

$$Nu = C\,Re^n Pr^m \tag{A.2}$$

The constants (C, n and m) were obtained by adopting a special calibration system in which we let the thermistor to move at different velocities (as will be described below) and the value of the current passing through the thermistor at each velocity was measured. The constants were determined by using curve fitting technique. Reynolds number was calculated at each defined position and the velocity of the flow was obtained as follows

$$U = \nu Re/De \tag{A.3}$$

where

$$De = (De_1 + De_2)/2$$

De_1 is the equivalent diameter where the flow is perpendicular to themistor's frontal area (see Fig. 2).

De_2 is the equivalent diameter where the flow is perpendicular to the thermistor's side area. It was found as follows

$$De_2 = 4 \times \text{flow area/wetted perimeter}$$

or

$$De_2 = \frac{4De_1((a+b)/2)}{2(De_1 + ((a+b)/2))}$$

where $a = 1.5$ mm and $b = 2.5$ mm as shown in Fig. 2.

A.3. The special calibration system

In order to estimate the constants of Eq. (A.2), a special calibration system was built. It consists of multi-speed carriage that was mounted over the water channel. The linear speed of the carriage was controlled by means of a rheostat which controls the voltage drop across the motor of the carriage. The velocity of the thermistor which was fixed to the carriage was determined by dividing the linear distance traveled by the carriage by the elapsed time interval that was measured by a stop watch.

References

[1] A.A. Kendoush, Hydrodynamics and heat convection from a disk facing a uniform flow, in: 2004 ASME Heat Transfer/Fluids Engineering Summer Conference, Charlotte, North Carolina, USA, July 11–15, 2004, Paper No. HT-FED2004-56797.
[2] D. Marshall, T.E. Stanton, On the eddy system in the wake of flat circular plates in three-dimensional flow, Proc. Roy. Soc. London A 130 (1930) 295–301.
[3] G.I. Taylor, Formation of a vortex ring by giving an impulse to a circular disk and then dissolving it away, J. Appl. Phys. 24 (1953) 104.
[4] T. Carmody, Establishment of the wake behind a disk, ASME J. Basic Engrg. 86 (1964) 869–882.
[5] J.R. Calvert, Experiments on the flow past an inclined disk, J. Fluid Mech. 29 (1967) 691–703.
[6] J.H. Vincent, Electrostatic precipitation of airborne dust in the wake of a perforated plate, J. Phys. D: Appl. Phys. 4 (1971) 1499–1512.
[7] T. Miyagi, T. Kamei, The standing vortex behind a disk normal to uniform flow at small Reynolds number, J. Fluid Mech. 134 (1983) 221–230.
[8] H.H. Sogin, Sublimation from disks to air streams flowing normal to their surfaces, ASME Trans. 80 (1958) 61–71.
[9] S.A. Beg, Forced convective mass transfer from circular disks, Warme und Stoffubertragung 6 (1973) 45–51.
[10] E.M. Sparrow, G.T. Geiger, Local and average heat transfer characteristics for a disk-situated perpendicular to a uniform flow, ASME J. Heat Transfer 107 (1985) 321–326.
[11] S.I. Kanbour, An investigation of thermal mixing of a stratified stream resulting from introduction of rigid barrier to the flow, PhD thesis, University of Maryland, 1970.
[12] BS 1041: Part 3: Temperature Measurement Guide to selection and use of industrial resistance thermometers, British Standards Institution, 1989.
[13] A.W. Izzat, Determination of the heat transfer parameters in the wake region of a circular disk, MSc thesis, College of Engineering, University of Baghdad, 1998.
[14] F.A. Schraub, S.J. Kline, J. Henry, P.W. Runstadler, A. Littell Jr, Quantitative determination of time dependent velocity fields in low speed water flows, ASME J. Basic Engrg. 87 (1965) 429–437.
[15] K. Lee, H. Barrow, Some observations on transport processes in the wake of a sphere in low speed flow, Internat. J. Heat Mass Transfer 8 (1965) 403–409.
[16] A.A. Kendoush, Low Prandtl number heat transfer to fluids flowing past an isothermal spherical particle, Internat. J. Heat Fluid Flow 16 (1995) 570–579.
[17] A.A. Kendoush, Calculation of flow resistance from a spherical particle, Chem. Engrg. Process. 39 (2000) 81–86.
[18] M. Sibulkin, Heat transfer at the rear and forward stagnation points of a body of revolution, J. Aeronaut. Sci. 19 (1952) 570–577.
[19] W.W. Short, Local convective heat transfer from a sphere, PhD thesis, California Institute of Technology, 1958.
[20] D.B. Murray, C. Ramirez, S. Holleran, Experimental study of convection in the wake of an inclined rectangular plate, in: Proceedings of the 12th International Heat Transfer Conference, 18–23 August, Grenoble, 2002.